THERMO-MECHANICAL BEHAVIOR OF A THERMOPLASTIC REINFORCED WITH DISCONTINUOUS GLASS FIBERS

Delphine Lopez[1], Sandrine Thuillier[2] and Yves Grohens[3]

[1] Univ. Bretagne Sud, FRE CNRS 3744, IRDL, F-56100 Lorient, France, delphine.lopez@univ-ubs.fr and www.irdl.fr
[1] Renault SAS, 1 Avenue du Golf, 78280 Guyancourt, France
[2] Univ. Bretagne Sud, FRE CNRS 3744, IRDL, F-56100 Lorient, France, sandrine.thuillier@univ-ubs.fr and www.irdl.fr
[3] Univ. Bretagne Sud, FRE CNRS 3744, IRDL, F-56100 Lorient, France, yves.grohens@univ-ubs.fr and www.irdl.fr

Keywords: Glass fiber reinforced thermoplastic, Thermo-mechanical behavior, Elasto-visco-plastic model, Parameter identification

ABSTRACT

Injected thermoplastics reinforced with discontinuous fibers have been widely used for several years in the automotive industry to reduce weight and then CO_2 emissions. The structural parts must maintain their geometrical shape under specific thermo-mechanical conditions and one of the challenges related to the use of such material is to have a reliable virtual design of industrial parts. These materials exhibit a non-linear mechanical behavior, partially reversible, anisotropic and time- and temperature-dependent. This study is focused on finding a good representation of the mechanical behavior over a temperature range from ambient temperature up to 85°C, using two models already presented in the literature, and based on an elasto-visco-plastic framework. Parameter identification is performed with an inverse approach over an experimental database consisting of tensile tests, both monotonous ones up to rupture at different strain rates, complex ones involving loadings-unloadings and relaxation steps and creep tests. The ability of the two models to represent all these tests is compared and the thermal evolution of the material parameters is analysed.

1 INTRODUCTION

Thermoplastics reinforced by discontinuous fibers are commonly used in the automotive industry for semi-structural applications like font-end module or tailgate [1,2] to reduce the vehicles weight and therefore CO_2 emissions. Such parts, made from polyamide [3] or polypropylene matrices [4] reinforced with discontinuous glass fibers, are usually obtained by injection to reach high production rates at low costs. This process leads to strong fiber orientations, resulting in a highly anisotropic behavior of the reinforced material. Moreover, technical specifications consider the long-term use of the automotive under cyclic loadings [3], the crash resistance [2] and environmental conditions with temperature ranges in-between ambient temperature up to 100°C-150°C [5].

However, the virtual mechanical design of such parts is still a challenge, in the sense that the mechanical behavior of thermoplastics reinforced with discontinuous glass fibers is a rather complex one, involving anisotropy, viscosity effects at different time scales and non-reversible phenomenon under static loadings. Moreover, the strong temperature sensitivity of thermoplastics affects also the behavior of the composite, as shown for polyamide 6,6 [5] and polypropylene [6].

The injection process leads to a strongly heterogeneous distribution of the discontinuous fibers, both in the plane and through the thickness, that can be represented by the second-order orientation tensor introduced by Advani and Tucker [7]. One recent trend to represent the anisotropy of the mechanical properties is to use Mori-Tanaka micromechanical model [8] to calculate elastic moduli from the fiber orientation tensor. An average tensor can be calculated from the microstructure by X-ray tomography [9] or from numerical prediction of the injection process [4,10] and then introduced in the model. Apart

from elasticity, there is a general agreement to introduce non-reversible phenomena via a viscoplastic framework, using invariants of the strain tensor [9] or internal variables [10]. Dean et al. [11] propose a model based on strain invariants and non-associated plasticity. Overall, a very close representation of stress-strain curves under several loading conditions is obtained in these three studies.

Few studies are dedicated to the prediction of the thermo-mechanical behavior of reinforced thermoplastics. Zhai et al. [6] investigate the decrease of Young's modulus with an increasing temperature, for unidirectional fiber glass-polypropylene composites and show that a power-law dependence, based on the melting temperature of the matrix, can well reproduce the decrease. Concerning the non-linear or viscous behavior, Launay et al. [5] identify the material parameters of their model (referred here as Launay's model) at several temperatures and analyse their evolution as a function of the difference between the test temperature and the glass transition temperature. Dean et al. [11] propose a linear dependence of some material parameters with the test temperature and predict accurately the stress levels at ambient temperature and 130°C for several orientations.

In this study, two phenomenological models are considered and emphasis is given to the thermal dependence. The material is made of a polypropylene matrix reinforced by discontinuous glass fibers, with a fixed fiber volume fraction. As a first step, anisotropy is not taken in account, by focusing on a given fiber orientation and a fixed tensile direction. Material parameters are identified with an inverse methodology at three temperatures and predicted stress-strain curves are compared with experimental data, for various loading conditions (monotonic loading, relaxation and creep tests).

2 MECHANICAL MODELS

Two mechanical models are considered, first a classical one implemented in standard in the finite element code Abaqus. The main advantage of this model is to have a reduced number of material parameters, though introducing three main characteristics of the mechanical behavior, e.g. elasticity, viscoplasticity (with no threshold) and time-independent plasticity. The second one is Launay's model selected for its high capacity to predict the mechanical behavior in a similar strain range as the one of the present study, over a very large experimental database. The general framework of large strain deformation is not recalled here and a 1D formulation is presented out of simplicity's sake.

2.1 Elasto-viscoplastic model (EVP model)

Two internal variables are considered, i.e. the viscoplastic strain ε^{vp} and the plastic strain ε^{p} and the total strain ε is calculated from:

$$\varepsilon = \varepsilon^{e} + \varepsilon^{p} + \varepsilon^{vp} \tag{1}$$

where ε^{e} is the elastic strain.
The Cauchy stress is derived from Hooke's law, using Young's modulus E:

$$\sigma = E\,\varepsilon \tag{2}$$

and the yield stress σ_Y is a threshold above which the plastic strain starts increasing:

$$\sigma \geq \sigma_Y\,, \dot{\varepsilon}^{p} = \dot{\lambda} \tag{3}$$

where λ is the plastic multiplier. Isotropic hardening is considered:

$$\sigma_Y = \sigma_O + Q\left(1 - \exp(-\,b\,\varepsilon^{p})\right) \tag{4}$$

Finally, the viscoplastic contribution is written as a time hardening term:

$$\dot{\varepsilon}^{vp} = A\sigma^{n}t^{m} \tag{5}$$

This model can be schematically represented by a threshold (evolving with the plastic strain) and a Maxwell element in series. It depends on 7 material parameters, i.e. $E, \sigma_O, Q, b, A, n, m$.

2.2 Launay's model

Launay's model, detailed in 3D and 1D formulations in [10], is recalled here without taking elastic softening into account. It depends on four internal variables ε^{vp}, ε^{ve1}, ε^{ve2} and α with the total strain calculated from:

$$\varepsilon = \varepsilon^{e} + \varepsilon^{ve1} + \varepsilon^{ve2} + \varepsilon^{vp} \tag{6}$$

Two viscoelastic branches, depending on four material parameters $(\eta_i, \tau_i), i = 1,2$ are in series with a viscoplastic branch and a spring. Moreover, non-linear kinematic hardening is considered for the viscoplastic contribution, as well as hyperbolic sine for the strain rate dependence. The following equations summarize the model:

$$\sigma = E\,(\varepsilon - \varepsilon^{ve1} - \varepsilon^{ve2} - \varepsilon^{vp}) \tag{7}$$

$$X = -\frac{2\,C\,\alpha}{3} \tag{8}$$

$$\dot{\varepsilon}_{vei} = \frac{\sigma}{\eta_i} - \frac{\varepsilon_{vei}}{\tau_i}\,, i = 1,2 \tag{9}$$

$$\dot{\varepsilon}_{vp} = A\left[\sinh\left(\frac{\left|\sigma - \frac{3\,X}{2}\right|}{H}\right)\right]^{m} \operatorname{sign}\left(\sigma - \frac{3\,X}{2}\right) \tag{10}$$

$$\dot{\alpha} = -A\left[\sinh\left(\frac{\left|\sigma - \frac{3\,X}{2}\right|}{H}\right)\right]^{m} \left(sign\left(\sigma - \frac{3\,X}{2}\right) + \gamma\,\alpha\right) \tag{11}$$

There is a total of 10 parameters to identify, i.e. $E, C, \gamma, \eta_1, \tau_1, \eta_2, \tau_2, A, H, m$.

3 MATERIAL PARAMETER IDENTIFICATION

Tensile tests are carried out on an electro-mechanical testing machine with a load cell of maximum capacity 10 kN. Standard bone-shaped samples are cut from an injected rectangular plate, with a thickness of 2.75 mm [4]. The distance between the fixed grip and the moving one is initially set at 108 mm. The local displacement is measured with an extensometer of 25 mm gauge length set in the middle of the sample. Monotonic tests up to rupture are performed at an almost constant strain rate, ranging from 10^{-5} s^{-1} up to 10^{-3} s^{-1}. In addition, complex cycles made of loading and unloading steps at several strain levels followed by relaxation steps as well as creep tests under different stress levels are performed. For each configuration, at least 2 samples are tested to ensure the reproducibility. All the tests are performed on samples cut at several locations on the plate, thus corresponding to different fiber orientations, with respect to the tensile direction [12]. However, as the focus of this study is the thermal dependence of the mechanical behavior, only the most oriented configuration is considered here. The glass transition temperature T_g of the composite is determined equal to 0°C, with dedicated Dynamic Mechanical Analysis. Isothermal tests are conducted at three temperatures above T_g, e.g. ambient temperature, 60°C and 85°C. At 60°C, only tensile test up to rupture and loading-unloading-relaxation tests are available in the database. It should be emphasized that the maximum strain at rupture is around 3% whatever the temperature. However, stress-strain curves are intentionally cut at 1.8% in the database, with respect to the industrial application. Moreover, relaxation steps are applied with an imposed and constant displacement of the grips, leading to small variations of the extensometer displacement, as highlighted in Fig. 1.

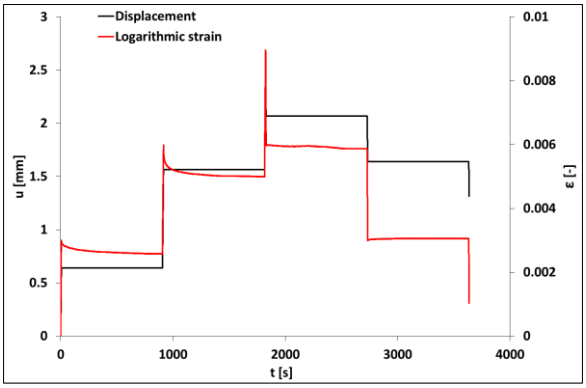

Figure 1: Displacement (u) and logarithmic strain (ε) evolutions as a function of time during a loading-unloading-relaxation test performed at a strain rate of 10^{-4} s^{-1}

A dedicated software SiDoLo, developed at IRDL [13], is used to implement and integrate the constitutive equations of each model and to also perform inverse identification of the material parameters. The identification scheme is based on an inverse approach corresponding to an optimization process, which main goal is to seek for a set of material parameters leading to a small gap between the experimental observations and the numerical results. This gap is evaluated with a cost function defined in the least square sense, normalized by the experimental values and with a possibility to weight the different tests. Output data used to calculate the cost function can be stress levels, in case of monotonic or relaxation tests or strain levels for creep tests. In order to minimize the cost function, the Levenberg-Marquardt gradient-based algorithm is used (e.g. [13]).

For both models, the following procedure is used: material parameters are identified at each temperature. Young's modulus and the yield threshold for EVP model are limited within ranges derived from the experimental results. A first identification is performed using creep tests. Then, loading-unloading-relaxation tests are added to the database and finally tests up to rupture, at several strain rates. This procedure is followed at ambient temperature and 85°C. Then, limits are fixed at 60°C to obtain a monotonous variation, as found previously [5] above T_g. Several initial parameter sets are tried, to avoid local minima of the cost function. For both models, the identification allows only positive values for the parameters except *m* of EVP model which is strictly negative and limited to -1. In addition, the factor --*m*/*n* must be inferior to 1. Due to the rather large number of material parameters, uniqueness of the optimized parameter set for Launay's model is not guaranteed and further analysis is needed.

4 RESULTS AND DISCUSSION

The capacity of the two models to simulate physical contributions such as viscosity, hardening, hysteresis and time-dependence are compared at different temperatures.

3.1 Strain rate effect

The strain rate effect is evidenced with tensile tests performed up to rupture. Figs. 2 and 3 show the experimental evolution of Cauchy stress with the logarithmic strain, limited to 2%, obtained at ambient temperature and 85°C for different strain rates. Numerical predictions of EVP and Launay's models are also displayed. The impact of the strain rate is rather weak but non-negligible with a variation around 5% in term of stress between three different strain rates. The temperature effect is clearly observed with a diminution by 2 of the maximum stress level reached during the test. This specificity is well reproduced by the two models. Launay's model gives a good prediction of the stress levels whatever the temperature whereas EVP model underestimates the stress level at 85°C. Overall, Launay's model offers very satisfying predictions for each configuration. On the contrary, EVP model has more difficulties to capture the strain rate effect, especially at higher strains. Moreover, the threshold of the elastic-plastic transition is clearly visible because of a sudden change of slope occurring when the elastic limit is reached. Therefore, the non-linear material behavior is less properly simulated. The same trend is also

observed at 60°C for each model though the result is not displayed here.

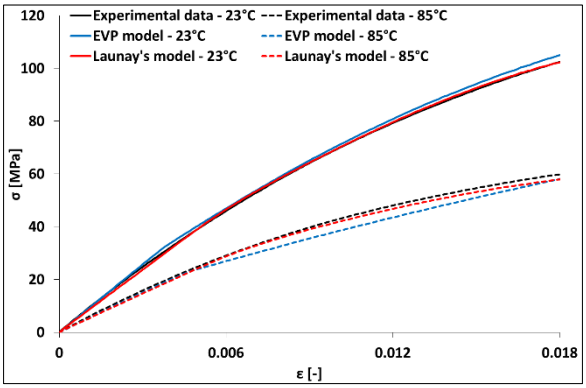

Figure 2: Experimental and simulated stress-strain curves of tensile tests performed up to rupture at ambient temperature and 85°C at a strain rate of 10^{-4} s^{-1}

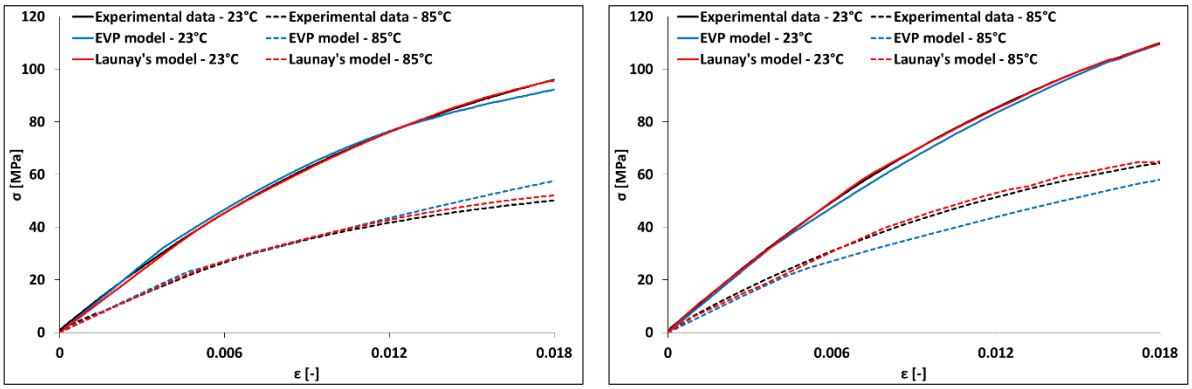

(a) **(b)**

Figure 3: Experimental and simulated stress-strain curves of tensile tests performed up to rupture at ambient temperature and 85°C, at strain rates of 10^{-5} s^{-1} (a) and 10^{-3} s^{-1} (b)

3.2 Short-term behavior

Figs. 4 and 5 show stress-time and stress-strain curves of loading-unloading tests interrupted by relaxations of 15 minutes at 3% and 5% of strain at the three temperatures.

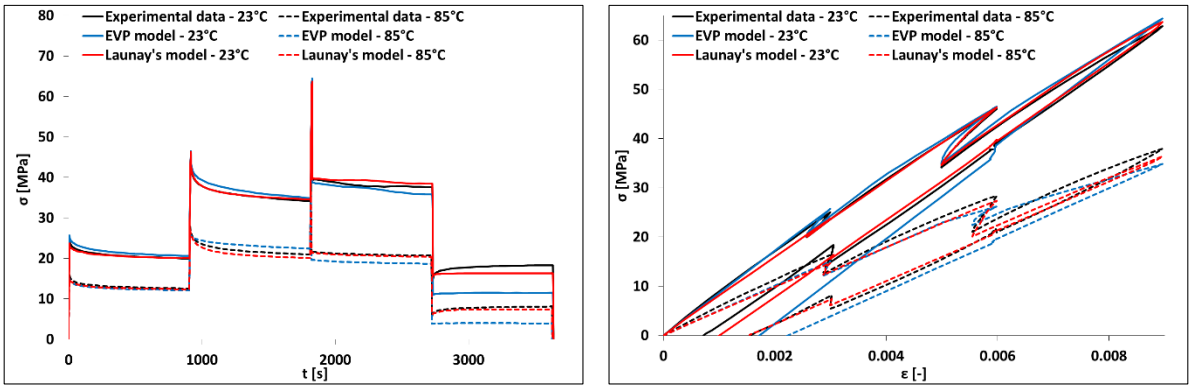

(a) **(b)**

Figure 4: Experimental and simulated stress-time (a) and stress-strain (b) curves of loading-unloading-relaxation tests at ambient temperature and 85°C obtained with a strain rate of 10^{-4} s^{-1}

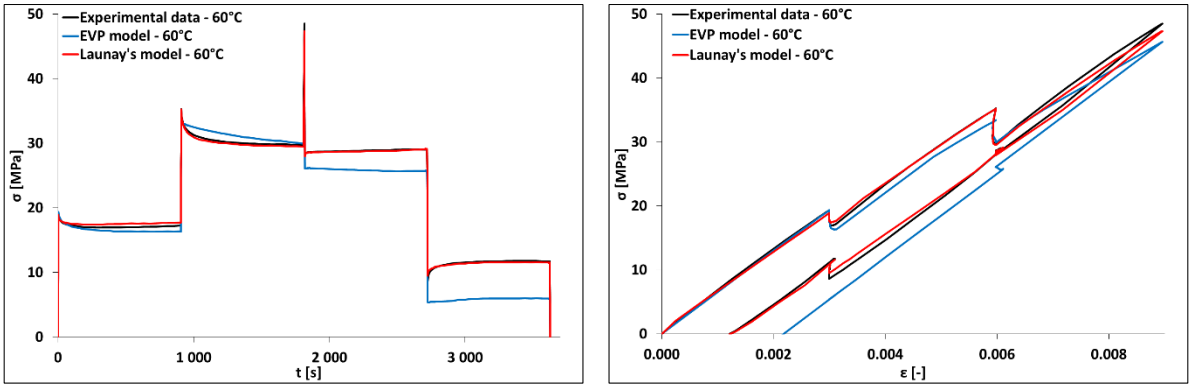

Figure 5: Experimental and simulated stress-time (a) and stress-strain (b) curves of loading-unloading-relaxation tests at 60°C obtained with a strain rate of 10^{-4} s^{-1}

It can be seen that EVP model gives a close enough prediction during loading path, except for the maximum stress level reached during the test. The main limitation of EVP model results in the difficulty to obtain a significant stress relaxation and reach the maximum stress level of the test with the same material parameters. In addition, it is noticed that for the last relaxation during the unloading path, the experimental stress is increasing. EVP model is not able to simulate this characteristics also observed in [9] whereas Launay's model captures it quite perfectly. Moreover, EVP model underestimates significantly the stress relaxation during unloading, especially at 60°C, leading to an important overestimation of the residual strain. Relative gap of residual strain prediction for EVP model at 60°C is close to 75% at 60°C, and above 60% at 85°C, contrary to Launay's model which is near 0% whatever the temperature. At ambient temperature, the maximum stress level is well predicted and therefore a relative gap of 20% is obtained for Launay's model and more than 100% for EVP model.

3.5 Long-term behavior

The long-term behavior of the material is investigated by means of creep tests in tension. Fig. 6 shows results obtained at ambient temperature and 85°C under 20 MPa and 30 MPa for 4 hours.

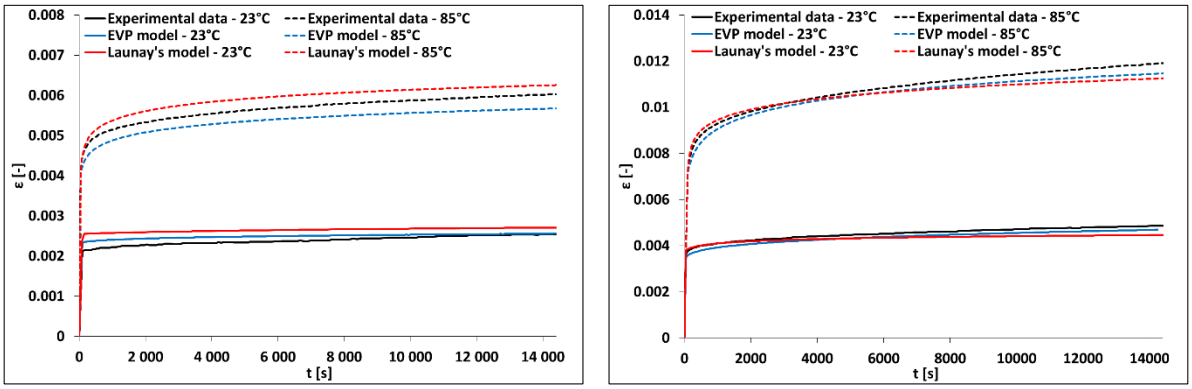

Figure 6: Experimental and simulated strain-time curves of creep test under 20 MPa (a) and 30 MPa (b) at ambient temperature and 85°C

Under 20 MPa at 85°C, the material behavior is well described in terms of kinetics by the two models but the strain evolution is not satisfying despite its very weak level. Under the highest stress, Launay's model overestimates the strain level whereas EVP model result is too low. Under the highest loading,

the predictions of both models are much better at each temperature. Launay's model captures well the beginning of the experimental curves whereas EVP model is closer at the end. On the contrary to previous tests, the two models are perfectly able to simulate correctly creep tests at different temperatures, strain rates and under several loadings.

3.5 Thermo-dependence of material parameters

The evolution with temperature of material parameters for EVP model is analyzed in this section. Fig. 7 shows the temperature dependence of Young's modulus, initial yield stress and hardening parameters. A sharp decrease of Young's modulus is obtained, consistent with the experimental results. Overall, all the parameters decrease when the temperature increases. Voce's law, commonly used for metallic materials, is used in order to contribute easily to the non-linear description of the material behavior. Nevertheless, the considered strain range is very low and therefore an isotropic linear hardening law could be sufficient, especially at elevated temperatures. Variation of each parameter is monotonous but no-linearity of the thermo-dependence is evidenced, more particularly for the viscoplastic parameters Fig. 8. The parameter A has a very low value at ambient temperature and increases significantly at higher temperature. As shown from previous results, EVP model can predict creep rather well but it has strong difficulties to find a balance between short- and long-term behavior. The temperature is an additional constraint which highlights once more the model limitations. With optimized parameters at ambient temperature, viscous term brings a higher contribution than the plastic one, particularly at high strains, which is no longer observed at 85°C. Concerning Launay's model, a monotonous thermo-dependence of the parameters is also obtained.

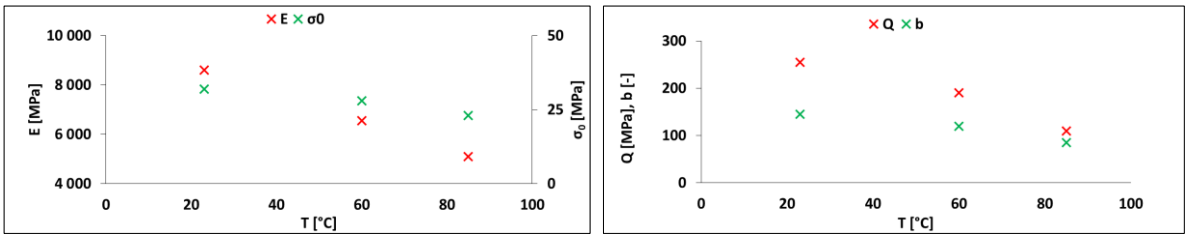

Figure 7: Variation of E, σ_O, Q, b with temperature.

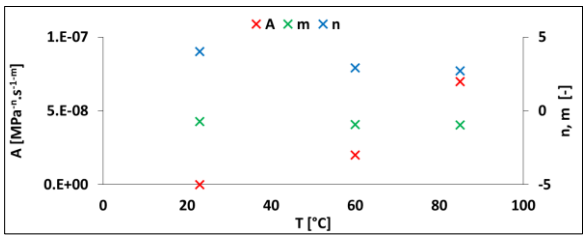

Figure 8: Variation of A, n, m with temperature

5 CONCLUSIONS

This study deals with the thermo-mechanical behavior of a composite made of discontinuous glass fibers in a thermoplastic matrix. Such a behavior shows several contributions: anisotropy, viscosity, non-reversible phenomenon and thermal dependence. An experimental investigation at several temperatures and strain rates, involving relation and creep tests, is performed. As a first step, only one orientation is considered, with the fibers mainly oriented in the tensile direction, to focus on the thermal dependence. Two phenomenological models are considered and the material parameters are identified using an inverse methodology over the whole database and at each temperature. Results consist of a comparison of experimental and predicted stress-strain data and their evolution with time as well as the evolution of the material parameters with the temperature. A good representation of the thermo-mechanical behavior with Launay's model is obtained.

ACKNOWLEDGEMENTS

The authors are indebted to Renault Technocentre for their financial support and for providing the material. ANRT is also acknowledged by the authors.

REFERENCES

[1] Schijve, 'Common errors and honest materials comparison for long glass PP materials', in *International AVK conference for reinforced plastics and thermoset molding compounds*, Baden-Baden, 2002, pp. 17–18.

[2] N. Bessières, 'Implantation d'une Approche Anisotrope dans le Dimensionnement Numérique des pièces Plastiques', in *SIA Conference Proceedings*, Paris-Saclay, 2017.

[3] A. Launay, Y. Marco, M. H. Maitournam, I. Raoult, and F. Szmytka, 'Cyclic behavior of short glass fiber reinforced polyamide for fatigue life prediction of automotive components', *Procedia Eng. Conf. Proc.*, vol. 2, no. 1, pp. 901–910, 2010.

[4] D. Lopez, S. Thuillier, Y. Grohens, and N. Bessières, 'Anisotropic Mechanical Behavior of an Injection Molded Short Fiber Reinforced Thermoplastic', in *AIP Conference Proceedings*, Nantes, 2016, vol. 1769, p. 60007.

[5] A. Launay, Y. Marco, M. H. Maitournam, and I. Raoult, 'Modelling the influence of temperature and relative humidity on the time-dependent mechanical behaviour of a short glass fibre reinforced polyamide', *Mech. Mater.*, vol. 56, pp. 1–10, 2013.

[6] Z. Zhai, C. Gröschel, and D. Drummer, 'Tensile behavior of quasi-unidirectional glass fiber/polypropylene composites at room and elevated temperatures', *Polym. Test.*, vol. 54, pp. 126–133, 2016.

[7] S. G. Advani and C. L. Tucker III, 'The use of tensors to describe and predict fiber orientation in short fiber composites', *J. Rheol.*, vol. 31, no. 8, pp. 751–784, 1987.

[8] T. Mori and K. Tanaka, 'Average stress in matrix and average elastic energy of materials with misfitting inclusions.', *Acta Metall.*, vol. 21, no. 5, pp. 571–574, 1973.

[9] A. Andriyana, N. Billon, and L. Silva, 'Mechanical response of a short fiber-reinforced thermoplastic: Experimental investigation and continuum mechanical modeling', *Eur. J. Mech. - ASolids*, vol. 29, no. 6, pp. 1065–1077, 2010.

[10] A. Launay, M. H. Maitournam, Y. Marco, I. Raoult, and F. Szmytka, 'Cyclic behaviour of short glass fibre reinforced polyamide: Experimental study and constitutive equations', *Int. J. Plast.*, vol. 27, no. 8, pp. 1267–1293, 2011.

[11] A. Dean, J. Reinoso, S. Sahraee, and R. Rolfes, 'An invariant-based anisotropic material model for short fiber-reinforced thermoplastics: Coupled thermo-plastic formulation', *Compos. Part Appl. Sci. Manuf.*, vol. 90, pp. 186–199, 2016.

[12] D. Lopez, S. Thuillier, and Y. Grohens, 'Thermo-mechanical anisotropic behavior of discontinuous glass fiber reinforced thermoplastic, submitted for publication', *Polym. Test.*, 2017.

[13] A. Andrade-Campos, S. Thuillier, P. Pilvin, and F. Teixeira-Dias, 'On the determination of material parameters for internal variable thermoelastic–viscoplastic constitutive models', *Int. J. Plast.*, vol. 23, no. 8, pp. 1349–1379, 2007.